

Augmented Reality Visualization of Joint Movements for Rehabilitation and Sports Medicine

Henrique Galvan Debarba¹, Marcelo Elias de Oliveira¹, Alexandre Lädermann^{2,3,4},
Sylvain Chagué¹ and Caecilia Charbonnier¹

¹ Artanim Foundation, Meyrin, Switzerland

² Faculty of Medicine, University of Geneva, Geneva, Switzerland

³ Division of Orthopedics and Trauma Surgery, La Tour Hospital, Meyrin, Switzerland

⁴ Division of Orthopaedics and Trauma Surgery, Clinique La Colline, Geneva, Switzerland

Abstract—We present a visualization tool for human motion analysis in augmented reality. Our tool builds upon our previous work on joint biomechanical modelling for kinematic analysis, based on optical motion capture and personalized anatomical reconstruction of joint structures from medical imaging. It provides healthcare professionals with the *in situ* visualization of joint movements, where bones are accurately rendered as a holographic overlay on the subject – like if the user has an “X-ray vision” – and in real-time as the subject performs the movement. The tool also provides a recording mechanism for the examination and acquisition of movements and range of motion information. Recorded information can be for instance retrieved at a later moment to assess patient’s progress in terms of kinematics during the rehabilitation phase. We also propose an intuitive non-sequential mean of navigating through recordings. It consists of pointing at movement trajectories for easy and intuitive retrieval of the meaningful portions of a movement. This tool allows for the *post hoc* replay and analysis of fast movements, such as from athletes movements in sports injury evaluation. Currently, hip and knee joints are supported.

Index Terms—augmented reality, visualization, calibration, joint kinematics, rehabilitation, sports medicine

I. INTRODUCTION

Healthcare professionals are interested in knowing how the range of motion (ROM) of the patient’s joint changes over time. This is true in a physical rehabilitation scenario, where the patient participates in periodic physical activities to recover movement, as well as in a post surgery scenario, where the physician wants to assess the effect of the intervention on the joint [1]. Patient’s physical examination usually includes palpation and evaluation of the passive ROM of the joint under investigation using standard goniometers or inclinometers [2], [3]. Unfortunately, this process may lack precision because the clinician has no direct access to the joint (i.e., external measurement). Moreover, when relying on passive ROM which are simple non-active motions, the clinician cannot always reproduce the movements that elicit the pain or cannot apprehend specific non-physiologic joint behavior during complex movements (e.g., sport activities).

We designed an augmented reality (AR) application for the personalized visualization and analysis of joint movements targeting several orthopedic activities, such as clinical examination, rehabilitation and sports injury evaluation and pre-

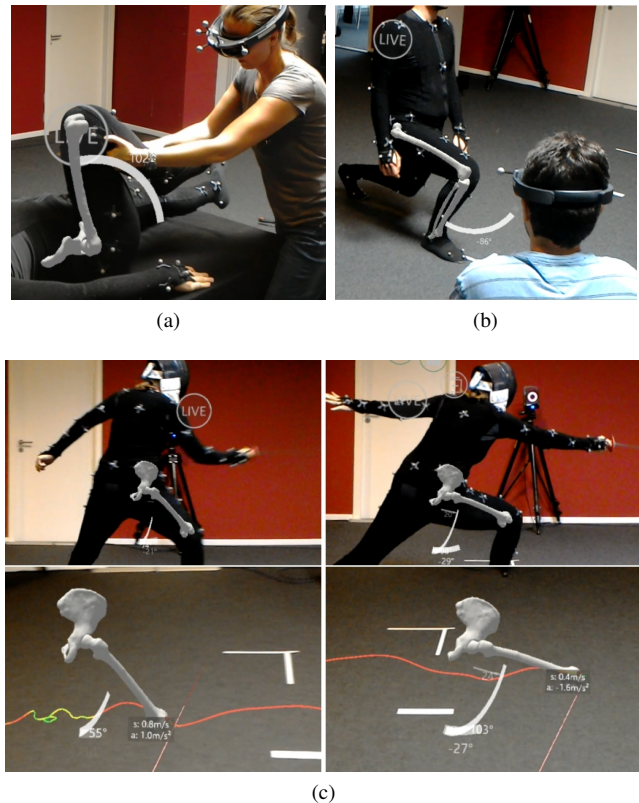


Fig. 1: Overview of our visualization application. In (a) and (b), we show the examination of the joint range of motion during passive and active movements, respectively. In (c), we show an athlete performing a fencing attack. Since this action is a fast movement difficult to observe and assess live (top), our system allows the replay of movements for posterior analysis (bottom). The user can add points to the surface of the bone to see its trajectory over time. By pointing towards the trajectory the user can then retrieve a posture and consult range of motion, speed and acceleration at that instant.

vention. Our application builds upon our previous work [4]–[6] on joint biomechanical modelling for kinematic analysis, based on optical motion capture and personalized anatomical reconstruction of joint structures from medical imaging. In

the application, the user can observe the movement of the bones, the ROM of the joint, and mark points on the surface of the bone to track their trajectory in space. All of this is accurately rendered as a holographic overlay on the subject – like if the user has an “X-ray vision” – and in real-time as the subject performs the movement (Fig. 1). Moreover, our application allows the *post hoc* analysis of fast movements by implementing a replay mechanism. The replay mode allows the detailed manipulation and visualization of clips recorded during the online visualization of joint movements. These movement clips can be moved in three dimensions, and we propose the use of trajectory lines as a means to navigate the recording in a non-linear fashion and quickly pick moments where meaningful ROM and kinematic (speed/acceleration) information are available.

The application was developed for the Microsoft HoloLens¹ Optical See-through Head-mounted Display (OST-HMD), which required the development of a calibration method to align the physical center of projection and optical axis of the OST-HMD to an arbitrary coordinate system defined by the external tracking system. The correctness of this alignment is critical as in an AR context a small error can result in major visual mismatch of the graphical overlay. Unlike related AR calibration [7], [8], our calibration method relies on matching movement data sets obtained through the external tracking system to the tracking solution built in the HoloLens.

In summary, the contributions of this paper are threefold: (i) development of an AR tool for medical applications, allowing accurate overlapping of personalized anatomical joint structures on top of the patient during motion; (ii) development of a non-sequential replay interface using trajectory lines to visualize recorded motion clips; (iii) development of a calibration method to align the physical center of projection of the HoloLens OST-HMD to the arbitrary coordinate system defined by the external tracking system.

II. RELATED WORK

AR is widely regarded as a valuable tool for medical applications since it allows the *in situ* visualization of inner-body organ systems. Researchers on the field have proposed AR systems for various applications, such as anatomy education [9], [10], medical training [11], physical rehabilitation [12], hepatic surgery planning [13], [14], forensic autopsy [15] and computer guided surgery [16], [17]. Moreover, AR has the potential to reinvent current medical care practices and the relation between health professionals and patients [18], [19], in particular for personalized medicine. This reality is closer than ever with the current surge of affordable AR capable devices, such as the Microsoft HoloLens.

In the context of joint movement visualization, Baillot et al. [20] proposed a knee kinematic simulation and posterior retrieval of pre-computed poses for AR visualization through a look-up table. The landscape of AR and computing have significantly changed since [20], and new kinematic models

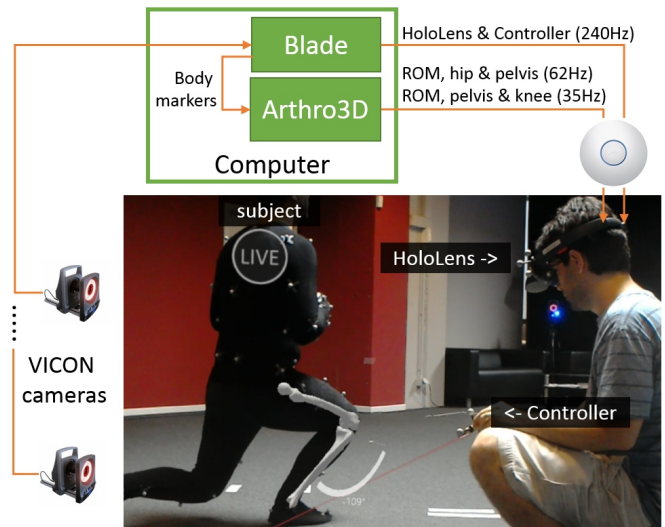


Fig. 2: Overview of the system architecture.

can be now computed and used to present joint poses in real-time [4]–[6]. To our knowledge, there is no study on the use of AR for medical visualization and examination of personalized joint kinematics to date. Such development is challenging as it requires expertise in different fields: motion capture, 3D reconstruction, biomechanical modeling, human computer interaction, and AR visualization.

III. MATERIALS AND METHODS

A. Equipment and System Architecture

The application hardware consists of a VICON MXT40S motion capture system², a computer (CPU: Intel Core i7-5960X, GPU: Nvidia GTX 980), and a Microsoft HoloLens OST-HMD. The VICON tracking system consists of 24 infrared cameras sampling at 240 Hz and is used to track retro-reflective markers attached to the subject (\varnothing 14 mm) and other auxiliary objects (\varnothing 19 mm). A dedicated hip or knee markers protocol [4], [6] is used to derive accurate joint kinematics from the subject.

A schematic representation of the system architecture is shown in Fig. 2. The VICON Blade software³ is used to process the cameras data and to stream the marker positions to Arthro3D, an in-house application for biomechanical simulation running on the same computer. Arthro3D receives the marker information and processes it with validated joint biomechanical models to reconstruct the poses of the body segments. Finally, Arthro3D streams the bone poses information and the joint ROM to the HoloLens through a wireless infrastructure. Two other auxiliary objects are tracked by the motion capture system, a controller used for interaction, and the HoloLens itself. These are directly streamed from Blade to the HoloLens. The HoloLens receives the poses of the tracked objects and is used for the projection and visualization of that information as an overlay on the patient.

²www.VICON.com

³www.VICON.com/products/software/blade

¹www.microsoft.com/en-us/HoloLens

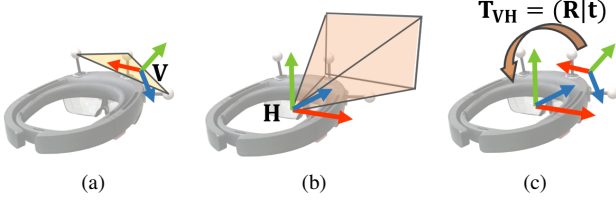


Fig. 3: (a) Coordinate system arbitrarily defined by optical markers rigidly attached to the AR headset. (b) Coordinate system of the AR headset used for camera projection. (c) The calibration determines the rigid transformation - rotation \mathbf{R} and translation \mathbf{t} - that aligns the tracked coordinate system to the AR camera coordinate system.

B. System Calibration

The HoloLens include optical and inertial sensors for position and orientation tracking. Although the algorithm combining these multi-sensors information in the HoloLens can yield estimations of the headset's pose in an absolute frame of reference, it may present several centimeters of error and is not appropriate for non-static backgrounds. Therefore, the AR headset tracking is combined with the VICON system to fulfill our application requirements.

With a set of markers placed in the HoloLens headset the VICON tracking can define an arbitrary coordinate system (Fig. 3a) with a position and orientation that do not match that of the AR headset image projection center (Fig. 3b). In order to correctly display the AR overlay in the headset, the rigid transformation that aligns the markers-based arbitrary coordinate system to the physical center of projection of the AR headset is required (Fig. 3c) and computed through a calibration procedure. High precision and accuracy are necessary, as small errors will affect the quality of the overlap of holographic and real objects. Note that the calibration will be valid as long as the coordinate system defined with the VICON tracking are preserved, i.e. if the physical markers and the registration of the coordinate system in the VICON system does not change, then the calibration can be used for multiple sessions. In addition, rendering with an AR headset requires a pair of cameras (stereo rendering pair), the position of both cameras are defined relative to the coordinate system shown in Fig. 3b by laterally translating the cameras by half of the interpupillary distance of the user.

1) *Calibration Procedure:* The mapping that express the center of projection \mathbf{H} relative to the coordinate system \mathbf{V} illustrated in Fig. 3 requires a rigid transformation with rotation \mathbf{R} and translation \mathbf{t} :

$$\mathbf{T}_{\mathbf{V}\mathbf{H}} = \begin{bmatrix} \mathbf{R} & \mathbf{t} \\ \mathbf{0}^T & 1 \end{bmatrix} \quad (1)$$

We obtain this transformation through a two steps calibration. In the first step, we record datasets with the headset poses from VICON and the HoloLens tracking. The user mounts the HoloLens and performs asymmetric translations along the

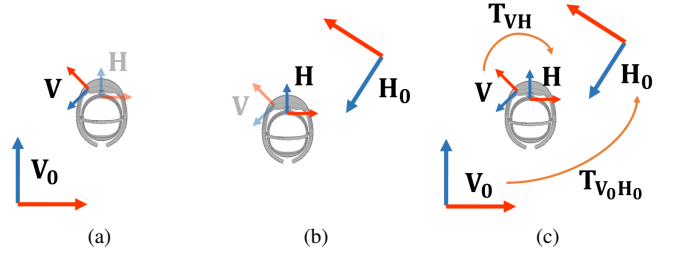


Fig. 4: Poses of the \mathbf{V} coordinate system are defined relative to VICON tracking origin \mathbf{V}_0 (a), while poses of the \mathbf{H} coordinate system are defined relative to the HoloLens tracking origin \mathbf{H}_0 (b). To find the calibration matrix $\mathbf{T}_{\mathbf{V}\mathbf{H}}$, we need to find the mapping $\mathbf{T}_{\mathbf{V}_0\mathbf{H}_0}$ from \mathbf{H}_0 to \mathbf{V}_0 so that \mathbf{H} can be represented in \mathbf{V}_0 , and \mathbf{V} can be represented in \mathbf{H}_0 (c). With $\mathbf{T}_{\mathbf{V}\mathbf{H}}$ known, the virtual camera can be set with respect to the VICON tracking origin using $\mathbf{T}_{\mathbf{V}_0\mathbf{H}} = \mathbf{T}_{\mathbf{V}_0\mathbf{V}} \cdot \mathbf{T}_{\mathbf{V}\mathbf{H}}$.

three axis of movement while rotations are avoided. The poses of the two tracked objects are represented in distinct coordinate systems, \mathbf{V} in \mathbf{V}_0 (Fig. 4a) and \mathbf{H} in \mathbf{H}_0 (Fig. 4b). To align their axis of movement (Fig. 4c), we need to estimate the rotation $\mathbf{R}_{\mathbf{V}_0\mathbf{H}_0}$ in $\mathbf{p}'_{h_i} = \mathbf{c}_v + \mathbf{R}_{\mathbf{V}_0\mathbf{H}_0} \cdot (\mathbf{p}_{h_i} - \mathbf{c}_h)$ that minimizes $E = \sum_{i=1}^n (\mathbf{p}_{v_i} - \mathbf{p}'_{h_i})^2$, where \mathbf{p}_v and \mathbf{p}_h are positions of \mathbf{V} and \mathbf{H} in \mathbf{V}_0 and \mathbf{H}_0 , and \mathbf{c}_v and \mathbf{c}_h are their respective centroids.

The matrix $\mathbf{R}_{\mathbf{V}_0\mathbf{H}_0}$ is obtained with the singular value decomposition (SVD) of the 3×3 covariance matrix $\mathbf{M} = \mathbf{P}_h \cdot \mathbf{P}_v^T$, where \mathbf{P}_h and \mathbf{P}_v are $3 \times n$ matrices whose the i -th column is obtained with $\mathbf{p}_{h_i} - \mathbf{c}_h$ and $\mathbf{p}_{v_i} - \mathbf{c}_v$, respectively. SVD gives $\mathbf{M} = \mathbf{U} \cdot \mathbf{\Sigma} \cdot \mathbf{V}^T$, where the optimal - in terms of minimizing the sum of squared errors - $\mathbf{R}_{\mathbf{V}_0\mathbf{H}_0}$ is given by $\mathbf{R}_{\mathbf{V}_0\mathbf{H}_0} = \mathbf{V} \cdot \mathbf{U}^T$ [21].

Consequently, the VICON and HoloLens trajectories can be aligned in terms of movement direction using the $\mathbf{R}_{\mathbf{V}_0\mathbf{H}_0}$ matrix. This allows us to estimate a linear mapping \mathbf{R}_i from the \mathbf{V} to \mathbf{H} for each corresponding point on the aligned trajectories with $\mathbf{R}_i = \mathbf{R}_{v_i}^T \cdot \mathbf{R}_{\mathbf{V}_0\mathbf{H}_0} \cdot \mathbf{R}_{h_i}$, where \mathbf{R}_{v_i} and \mathbf{R}_{h_i} refer to the \mathbf{V} and \mathbf{H} rotations at corresponding frames. Outlier rotations are removed based on the deviation of angle $\theta_i = \arccos(\frac{\text{trace}(\mathbf{R}_i) - 1}{2})$. We define inlier rotations as $Q_1 - IQR * 1.5 \leq \text{inliers} \leq Q_3 + IQR * 1.5$, where Q_1 and Q_3 are the first and third quartiles of the set of angles, and $IQR = Q_3 - Q_1$. The remaining rotations are converted into the quaternion representation \mathbf{q}_i , and their baricentric mean $\bar{\mathbf{q}}$ is used to approximate the average rotation \mathbf{R} [22].

In the second step, the headset is rigidly attached to a tripod, which allows for spherical movements around a spherical joint. We fit a sphere to each collection of positions \mathbf{p}_v and \mathbf{p}_h (positions of \mathbf{V} and \mathbf{H} coordinate systems). By subtracting the center of rotation from the positions, we obtain the $3 \times N$ matrices \mathbf{P}_v and \mathbf{P}_h , and each pair of poses can be used to build a $3 \times N$ matrix \mathbf{M} , with $\mathbf{M}_i = \mathbf{R}_{v_i}^T \cdot (\mathbf{R}_{\mathbf{V}_0\mathbf{H}_0} \cdot \mathbf{P}_{h_i} - \mathbf{P}_{v_i})$ for each i -th column of \mathbf{M} . Finally, the mean value of the rows of \mathbf{M} approximates the translation \mathbf{t} that defines the

physical center of projection of the headset relative to the VICON arbitrary tracker depicted in Fig. 3. As a result, we can build the rigid transformation $\mathbf{T}_{\mathbf{V}\mathbf{H}}$ in Equation 1. Note that this procedure depends on both HoloLens and VICON tracking, and is therefore susceptible to HoloLens tracking limitations when a small amount of data is used, optimal transformations can be obtained with the mean of several \mathbf{V} and \mathbf{H} pose correspondences in multiple recordings. Recordings were made by frame ($\approx 60\text{Hz}$), with the latest value of both tracking systems. As VICON tracking presents a higher latency, latency estimation and compensation was performed based on the cross-correlation of the movement speed of pairs of recordings.

2) *Assessing Calibration Quality*: The built-in camera of the HoloLens headset was used to estimate the projection error of the calibration procedure. The HoloLens overlays the camera image with the virtual scene as rendered for the right eye, capturing an image of the real environment that is superimposed by the virtual information. The HoloLens and a reference object were placed at the two ends of a 70 cm long rigid structure, both tracked using the VICON system. The reference object was placed so that a spherical marker on its center could be seen close to the center of the built-in HoloLens camera image. A virtual representation of the marker was rendered in the virtual space based on the tracked position of the reference object. The quality of calibration was assessed based on the overlap of the real marker with its virtual counterpart.

A total of 12 frames were randomly selected from a video with the rigid structure at 12 different orientations while at the center of the VICON tracking volume. Our results showed a mean absolute projection error of 3mm ($SD = 1\text{mm}$) between the real and virtual spheres.

C. Latency Compensation

Tracking systems have an intrinsic latency, which is further increased by network and the AR rendering pipeline, and affects the stability and accuracy of the superposition of real objects by holographic objects. For our system, we assessed a “motion to photon” latency of ≈ 50 ms. For instance, during a head rotation at the rate of 200° per second, 50 ms of latency yields an error of 10° in the hologram projection, resulting in a momentary superposition mismatch, and an overall perception that the holograms do not have a stable location in the real environment.

We adopt two approaches to mitigate this problem. One specific to the HoloLens, and a second one that is used in the live streaming of bone and controller poses. HoloLens tracking relies on inertial sensors that present smaller latency than optical tracking systems. Moreover, it also has built-in hardware used for post-render image deflection [23], [24], which accommodate the rendered image to the most recent pose available. To take advantage of these features, we align the coordinate systems of the VICON and HoloLens tracked camera poses, and use the most recent 50 ms interval of change in HoloLens pose as a complement to the current

VICON pose. Due to the variation on the number of frames, and therefore on the amount of HoloLens frames used, this yields a noisy approximation, which we address with an exponential smoothing. For other tracked objects in the scene (i.e., the bones and the controller), we predict future poses based on their current filtered estimate of position, rotation, linear velocity and angular velocity. An extended Kalman filter – implemented according to Welch and Bishop [25] – is employed to obtain these estimates. A prediction time of 30 ms is used, as artifacts became evident when compensating for longer intervals.

D. Biomechanical Simulation

Marker data streamed from VICON Blade software are retrieved in Arthro3D and are used to compute the 3D kinematics of the hip or knee joint. The major drawback with optical motion capture systems is that markers are placed on the skin surface and move relatively to the underlying bone during movement with the deformation of the soft tissues (i.e., soft tissue artifact (STA)), representing a critical source of errors [26].

To solve this issue, Arthro3D software integrates validated biomechanical joint models for the hip [4], [5] and knee [6] to compute accurate joint poses accounting for STA. The models are based on a subject-specific kinematic chain of two rigid bodies (for the hip, the pelvis and femur; for the knee, the femur and tibia) using personalized joint 3D models reconstructed from medical images. The optimal pose of the kinematic chain is obtained by using a global optimization algorithm (to minimize STA error globally [27]) and specific anatomical constraints (i.e., 6 DOFs joint models). The accuracy of the models developed range from 0.24 to 3.7 mm in translations and from 0.55° to 6° in rotations, which is acceptable for clinical use in the study of joint pathology [4]–[6]. More details about the models and their validation can be found in [4]–[6].

From the computed bone poses, the ROM of the hip and knee joints can be evaluated at each point of the movement. This is achieved by calculating the relative orientation between the pelvis and femur (or femur and tibia) using two local coordinate systems [5], which were established based on the definitions suggested by the International Society of Biomechanics [28] to represent the pelvic and femoral (or femoral and tibial) segments. Their relative orientations are finally decomposed into three successive rotations [29] to express the ROM in clinically relevant terms (i.e., flexion/extension, abduction/adduction and internal/external rotation).

As a result, the following information is streamed to the HoloLens: the computed bones poses and the computed joint ROM for the current frame. For the hip and knee joint simulation, each frame takes respectively ≈ 17 ms and ≈ 28 ms to be computed, resulting in a streaming frequency of ≈ 62 Hz and ≈ 35 Hz.

E. AR Application Design

1) *Live and Replay Subscenes*: The LIVE sub-scene allows clinicians to perform online *in situ* visualization and analysis of the joint movements, and to record movement clips as the subject performs the desired actions (Fig. 1ab). That is, with the subject-specific bone models reconstructed from medical imaging and simulated by our biomechanical simulation software, the user can visualize in real-time the movement of the hip or knee joint as an overlay on the subject. Mind that only one LIVE sub-scene exists as it is linked to the live performer and the clip recording tool.

A REPLAY sub-scene allows for detailed manipulation, visualization, analysis, and playback control of clips recorded in the LIVE sub-scene (Fig. 1c). While the LIVE sub-scene requires a tracked performer, REPLAY sub-scenes can be visualized during or after a motion capture session. For instance, the clinician can load scenes from past sessions to evaluate the patient’s progress or can visualize REPLAY sub-scenes without the subject. Numerous REPLAY scenes can be instantiated on demand based on the database of recorded clips for that subject.

2) *Visualization and Interaction Elements*: A 6 DOFs (position and rotation) controller is used for input. The controller is coupled with a HoloLens clicker, which connects directly to the headset and is used only as a confirmation button. A raycasting metaphor – where the pose of the controller controls the origin and direction of a laser pointer-like ray – is used to point and interact with the scene.

The interaction options of each sub-scene are disposed in radial menus. We preferred radial menus over traditional list or table-like option arrangements for two reasons: 1) similar effort is required to reach any of the radial menu options; and 2) they are relatively compact to visualize, which is adequate when a small field of view – such as that of the HoloLens OST-HMD which has a vertical field of view of $\approx 17^\circ$ – is available. Each sub-scene has its own menu, which is represented by a circle at the top of the 3D bone models. The user can show and hide the menu options by pointing to this circle and quickly pressing the controller button. Menu options can be activated in the same way. Note that the menu options are different for LIVE and REPLAY sub-scenes, the options are detailed in Fig. 5.

The clinician can visualize the current amount of flexion/extension, abduction/adduction and internal/external rotation of the joint under investigation, and add trajectory points to the surface of the bones. These tools are available in both LIVE and REPLAY sub-scenes. Fig. 1ab and Fig. 6a show the visualization of the angles in a LIVE sub-scene. Rendering opacity is proportional to the rotation angle, which prevents the angle from being visible when it is small, thus avoiding a cluttered virtual layer. Opacity has a linear relation with the rotation angle when it is smaller than 40° and becomes saturated for angles equal or above 40° .

Movement trajectories are drawn as line strips in 3D space (Fig. 1c and Fig. 6b), and the rendering color of their segments is defined by the speed of movement, and the speed to color

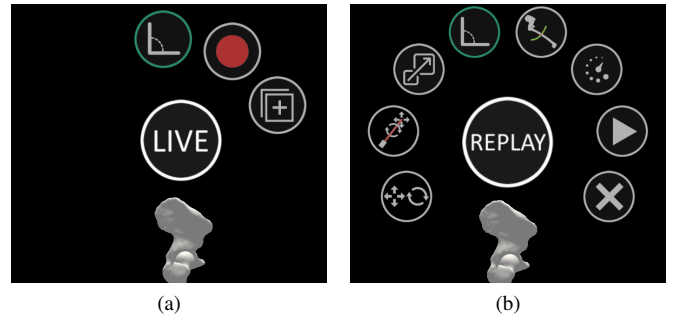


Fig. 5: Menu options of a LIVE sub-scene (a) are different than the options of a REPLAY sub-scene (b). In a LIVE sub-scene, the user can visualize the joint ROM, record motion clips, and create REPLAY sub-scenes from recorded motion clips – clockwise options in (a). In a REPLAY sub-scene, the user can rotate, translate and scale the sub-scene, visualize the joint ROM, replay the motion clip in a non-sequential or sequential way, and erase the sub-scene from the environment – clockwise options in (b).

mapping is dependent on the task. To add a trajectory point, the controller button should be clicked while the ray intersects with one of the bone models. Trajectory points added to a LIVE sub-scene show a limited interval of movement, and their placement positions are stored in clips for retrieval when a REPLAY sub-scene is generated. Trajectory points added to or loaded with REPLAY scenes present the movement of that point for the entire movement clip.

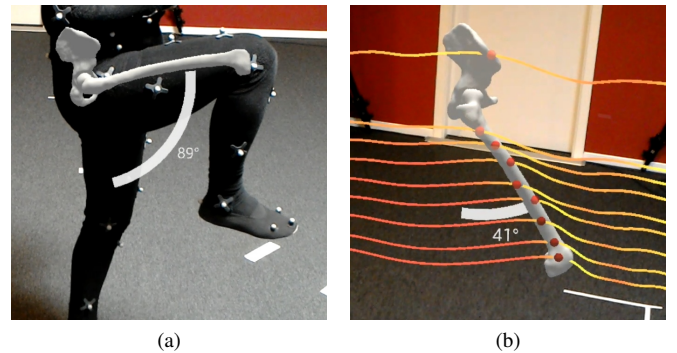


Fig. 6: Visualization of joint ROM (here, 89° of hip flexion) (a) and trajectories of a motion clip (b). Trajectories are created by points placed over the surface of the bone.

3) *3D Manipulation*: The user can translate, rotate, and uniformly scale a REPLAY sub-scenes using the controller. There are three menu options that activate different forms of manipulation (Fig. 7):

Hand-centered translation and rotation – the object translates and rotates according to controller movement as if attached to the tip of a rod that extends from the manipulator to the intersection point (Fig. 7b), as described in [30].

Intersection-centered translation and rotation – similar to the method described above, the object translates and rotates

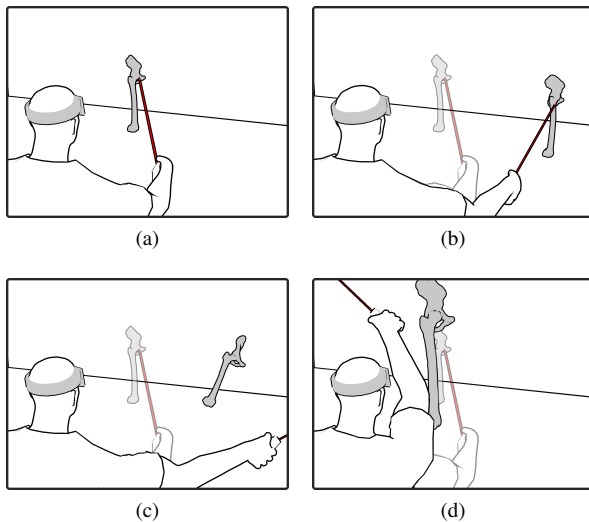


Fig. 7: The model in a REPLAY sub-scene (a) can be manipulated with three tools: (b) Hand-centered translation and rotation; (c) intersection-centered translation and rotation; and (d) uniform scale using vertical movements.

according to controller movement, but the center of rotation is now defined as the ray-casting intersection point at the moment when the manipulation started (Fig. 7c), as proposed in [30].

Uniform scale – the object is uniformly scaled by moving the controller upward to increase scale and downward to decrease scale (Fig. 7d).

When one of these options is selected in the REPLAY sub-scene menu, the user can point at one of the objects in that sub-scene and click and hold the controller button to start the manipulation. The manipulation is finalized when the button is released.

4) *Replay Manipulation*: The user can control the execution of a REPLAY sub-scene clip with three replay tools available from the menu:

Play and pause – The play button initiates the playback of the clip with recording speed, when selected it is replaced by a pause button.

Gesture-based sequential frame selection – When this tool is selected, the user can sequentially navigate through the frames of a clip by pressing and holding the button and rotating the controller around the axis defined by the ray. A clockwise rotation advances the frames forward, while a counter clockwise rotation navigates backward. The reproduction rate is of 1 second per 10° of rotation.

Trajectory-based non-sequential frame selection – It uses ray-casting to select a specific frame in the clip. The user presses and holds the button, and points the controlled ray towards the trajectories. For the duration of the button click, the trajectory point with the shortest ray to point distance is selected and used to retrieve and present the corresponding clip frame. The speed and acceleration of that point in the trajectory are also presented. This method allows for easy and fast selection of poses covering a large volume of space (Fig.

1c).

IV. USE SCENARIOS

The development of this application was accompanied by an experienced orthopedic surgeon. Moreover, a review session was performed with five medical specialists in the field of orthopedics to gather feedback. In this review, we presented the current state of our tool and discussed the use scenarios presented below.

Physical examination – The physical examination scenario considers a patient coming for a check-up, where the clinician usually asks him/her to perform standard passive (clinician-controlled) and active (patient-controlled) movements to assess the ROM of the joint. With our application, the clinician can qualitatively and quantitatively assess the joint ROM in real-time as the patient performs a specific task. He/she can also take pictures and record videos of the desired poses, and record movement clips for side by side comparison of passive vs. active ROM, or of ROM differences from a past session. Moreover, patients are often unable to perform some of the active movements with the desirable amplitude, or might feel discomfort at specific poses. These moments can be easily identified in the movement trajectory as the patient might interrupt the movement, or adopt a specific strategy in order to complete the movement by avoiding postures causing pain. By recording and observing movement clips, clinicians can use the trajectory to easily retrieve these frames and observe the state of the joint at that moment to better understand the functional problem. Pictures and videos from the session can be shared with other healthcare professionals treating the patient.

Physical rehabilitation – In the context of physical rehabilitation, our application could be used to evaluate ROM improvements resulting from physiotherapy sessions. The application can assist practitioners in keeping track of patient's improvement and generate more comprehensive documentation that can be used to help enhance patient's understanding of the treatment goals. In such cases, the patient could attend a monthly appointment where the clinician would use the LIVE mode of the application to observe the current ROM of the treated joint during typical rehabilitation exercises. The practitioner could record personalized videos that demonstrate the correct – and possibly incorrect – execution of the movement. These movies could be made available to patients for later consultation.

Sports medicine – In the context of sports medicine, an athlete suffering from pain during a common movement in his/her practice could benefit from our application. For instance, a fencing athlete may feel pain while performing a forward attack as he/she flexes and transfers weight to his/her advancing hip joint. The thorough analysis of such actions can help identify movements and poses that may possibly cause joint damage (here, one can suspect a hip impingement, i.e., an abutment between the femoral neck and the acetabular part of the pelvis [31], [32]), and thus prevent future injuries or lesions. However, conventional measurement tools cannot assess the dynamic ROM and abnormal functional behavior of

the joint during such actions. With our application, clinicians can record a clip as the subject performs the movement, and then review it by selecting the relevant points in the trajectory. Similarly to the physical examination scenario, clinicians can have a close look at the state of the joint as the movement develops.

During the review session, we walked the medical specialists through the functionalities of the application, and conducted a guided individual session. All users could easily access and understand the functionalities of the LIVE mode, where the only interaction required was the selection of options in the menu and the addition of trajectory points through raycasting. The use of the REPLAY mode added some complexity and had a steeper learning curve: two of the users could select and control all the pose and replay manipulation tools with ease, two of them had to try the pose manipulation tools a few times before they could succeed, while one user showed difficulties with the use of pose manipulation tools and the sequential frame selection.

V. DISCUSSION AND CONCLUSION

We presented an AR application for visualization of joint movements. This application can be used in the context of rehabilitation and sports medicine to offer healthcare practitioners with the *in situ* assessment of patient-specific joint kinematics, as well as the recording and replay of movement clips for posterior analysis. This paper also presented a calibration procedure to register the HoloLens OST-HMD with an external tracking system, allowing to accurately overlay on the subject his/her personalized anatomical joint structures.

The application was reviewed with five medical specialists. Overall, the most useful functionality was the visualization and display of joint ROM during live or replay actions, which brings a totally new way to conceive physical examination and understand underlying functional mechanisms. One of the interesting needs expressed by the medical specialists was the exchange of patient-specific information based on photo and video captures. Although not implemented as part of the application, these needs were addressed using the built-in photo and video recording functionalities of the HoloLens. With the guidance of an experienced orthopedic surgeon, we defined three use scenarios where our application could be a useful tool to improve current orthopedic examination procedures.

We acknowledge some limitations in the proposed system: first, our system currently requires expensive equipment and a complex markers protocol to derive accurate joint kinematics, which are two limiting factors that can prevent us from implementing this system at a larger scale or as a standard of care. Simplifications in terms of markers protocols, as well as the possibility of adopting a more cost- and space-efficient tracking solution will thus have to be investigated in order to export this system in clinics. Cheaper motion tracking alternatives, such as the Microsoft Kinect, have been used for rehabilitation activities [33], but is not reliable enough when the correctness of movement parameters are central

to the application, as assessed in [34]. Second, there are potential limitations to the accuracy of the global set-up. Indeed, errors can originate from two different sources: one source of error can be the calibration between the HoloLens and VICON system (error ≈ 3 mm when 70 cm away from the HoloLens). Another source of error can be the joint kinematics computation from motion capture data due to STA (translational error < 3.7 mm, rotational errors $< 6^\circ$). Despite these two possible sources of error, our methodology is still accurate, valid and acceptable for clinical use in the study of joint pathology [4]–[6]. In particular, we do believe that the error values of the global set-up does not call into question the usefulness of the system.

Future work will consider the extension of this system in different directions. Two short-term developments will be prioritized: first, we will support the visualization of the shoulder, another joint commonly affected by musculoskeletal disorders. This will require the adaptation of our biomechanical model for patient-specific shoulder kinematics [35] for use in real-time applications. Second, we will perform a comprehensive validation study with patients comparing our system with conventional methods of joint ROM examination. We also plan to explore the use of contextual *in situ* visualization rendering, which can facilitate depth perception of the AR overlay [36].

Moreover, we plan to support direct annotation of content. For instance, we could use our controller or hand recognition for drawing, as investigated by [37]. Mobile phones could also be evaluated as a replacement for the controller, introducing an input interface (touchscreen) that is familiar to the general audience. Touchscreen allows efficient data input and could be used for annotations and as an effective file management interface. Finally, the application could be made cross-platform so that recorded material, such as motion clips and general media files, could be reviewed and annotated at a later time directly on a mobile phone or tablet.

In conclusion, with the growing popularity of AR devices in the consumer market we believe that its presence in the medical field will become ubiquitous. Several literature reviews provide an account to the improvement in technology and application of AR in the medical [19], [38] and general [39]–[41] contexts. We argue that our system adds to the construction of this future by exploring the use of AR in novel orthopedic applications.

ACKNOWLEDGMENTS

We wish to thank the anonymous reviewers for their comments. This work was supported by La Tour Hospital and the clinics of Hirschlanden La Colline.

REFERENCES

- [1] A. Lädermann, P. J. Denard, J. Tirefort, F. C. Kolo, S. Chagué, G. Cunningham, and C. Charbonnier, “Does surgery for instability of the shoulder truly stabilize the glenohumeral joint?: A prospective comparative cohort study,” *Medicine*, vol. 95, no. 31, pp. e4369–e4369, 2016.
- [2] J. Moreside and S. McGill, “Quantifying normal 3d hip rom in healthy young adult males with clinical and laboratory tools: Hip mobility restrictions appear to be plane-specific,” *Clin Biomech*, vol. 26, no. 8, pp. 824–826, 2011.

- [3] S. Roach, J. S. Juan, D. Suprak, and M. Lyda, "Concurrent validity of digital inclinometer and universal goniometer in assessing passive hip mobility in healthy subjects," *Int J Sports Phys Ther*, vol. 8, no. 5, pp. 680–688, 2013.
- [4] C. Charbonnier, L. Assassi, P. Volino, and N. Magnenat-Thalmann, "Motion Study of the Hip Joint in Extreme Postures," *Vis Comput*, vol. 25, no. 9, pp. 873–882, 2009.
- [5] C. Charbonnier, F. Kolo, V. Duthon, N. Magnenat-Thalmann, C. Becker, P. Hoffmeyer, and J. Menetrey, "Assessment of Congruence and Impingement of the Hip Joint in Professional Ballet Dancers," *Am J Sports Med*, vol. 39, no. 3, pp. 557–566, 2011.
- [6] C. Charbonnier, S. Chagué, F. Kolo, V. Duthon, and J. Menetrey, "Multi-body Optimization with Subject-Specific Knee Models: Performance at High Knee Flexion Angles," *Comput Meth Biomech Biomed Eng*, vol. In Press, 2017.
- [7] M. Tuceryan, Y. Genc, and N. Navab, "Single-point active alignment method (spaam) for optical see-through hmd calibration for augmented reality," *Presence: Teleoperators and Virtual Environments*, vol. 11, no. 3, pp. 259–276, 2002.
- [8] L. Qian, E. Azimi, P. Kazanzides, and N. Navab, "Comprehensive tracker based display calibration for holographic optical see-through head-mounted display," *arXiv preprint arXiv:1703.05834*, 2017.
- [9] M. Meng, P. Fallavollita, T. Blum, U. Eck, C. Sandor, S. Weidert, J. Waschke, and N. Navab, "Kinect for interactive ar anatomy learning," in *2013 IEEE International Symposium on Mixed and Augmented Reality (ISMAR)*, Oct 2013, pp. 277–278.
- [10] T. Blum, V. Kleeburger, C. Bichlmeier, and N. Navab, "mirracle: An augmented reality magic mirror system for anatomy education," in *Virtual Reality Short Papers and Posters (VRW), 2012 IEEE*. IEEE, 2012, pp. 115–116.
- [11] T. Blum, S. M. Heining, O. Kutter, and N. Navab, "Advanced training methods using an augmented reality ultrasound simulator," in *2009 8th IEEE International Symposium on Mixed and Augmented Reality*, Oct 2009, pp. 177–178.
- [12] A. E. F. Da Gama, T. M. Chaves, L. S. Figueiredo, A. Baltar, M. Meng, N. Navab, V. Teichrieb, and P. Fallavollita, "MIRRABILITATION: A clinically-related gesture recognition interactive tool for an rehabilitation system," *Computer methods and programs in biomedicine*, vol. 135, pp. 105–114, 2016.
- [13] H. G. Debarba, J. Grandi, A. Maciel, and D. Zanchet, "Anatomic hepatectomy planning through mobile display visualization and interaction," in *MMVR*, vol. 173, 2012, pp. 111–115.
- [14] J. G. Grandi, A. Maciel, H. G. Debarba, and D. J. Zanchet, "Spatially aware mobile interface for 3d visualization and interactive surgery planning," in *Serious Games and Applications for Health (SeGAH), 2014 IEEE 3rd International Conference on*. IEEE, 2014, pp. 1–8.
- [15] T. Kilgus, E. Heim, S. Haase, S. Prüfer, M. Müller, A. Seitel, M. Fangerau, T. Wiebe, J. Iszatt, H.-P. Schlemmer *et al.*, "Mobile markerless augmented reality and its application in forensic medicine," *International journal of computer assisted radiology and surgery*, vol. 10, no. 5, pp. 573–586, 2015.
- [16] Y. Abe, S. Sato, K. Kato, T. Hyakumachi, Y. Yanagibashi, M. Ito, and K. Abumi, "A novel 3d guidance system using augmented reality for percutaneous vertebroplasty," *Journal of Neurosurgery: Spine*, vol. 19, no. 4, pp. 492–501, 2013.
- [17] H. Wang, F. Wang, A. P. Y. Leong, L. Xu, X. Chen, and Q. Wang, "Precision insertion of percutaneous sacroiliac screws using a novel augmented reality-based navigation system: a pilot study," *International orthopaedics*, vol. 40, no. 9, pp. 1941–1947, 2016.
- [18] T. Ni, A. K. Karlson, and D. Wigdor, "Anatome: facilitating doctor-patient communication using a projection-based handheld device," in *Proceedings of the SIGCHI Conference on Human Factors in Computing Systems*. ACM, 2011, pp. 3333–3342.
- [19] L. Chen, T. Day, W. Tang, and N. W. John, "Recent developments and future challenges in medical mixed reality," in *In Mixed and Augmented Reality (ISMAR), 2017 IEEE International Symposium on*, 2017, p. to appear.
- [20] Y. Baillet, J. P. Rolland, K.-C. Lin, and D. L. Wright, "Automatic modeling of knee-joint motion for the virtual reality dynamic anatomy (vrda) tool," *Presence: Teleoperators and Virtual Environments*, vol. 9, no. 3, pp. 223–235, 2000.
- [21] K. S. Arun, T. S. Huang, and S. D. Blostein, "Least-squares fitting of two 3-d point sets," *IEEE Transactions on Pattern Analysis and Machine Intelligence*, vol. PAMI-9, no. 5, pp. 698–700, Sept 1987.
- [22] C. Gramkow, "On averaging rotations," *Journal of Mathematical Imaging and Vision*, vol. 15, no. 1, pp. 7–16, 2001.
- [23] R. SO, "Compensating lags in head-coupled displays using head position prediction and image deflection," *Journal of Aircraft*, vol. 29, no. 6, pp. 1064–1068, 1992.
- [24] T. Mazuryk and M. Gervautz, "Two-step prediction and image deflection for exact head tracking in virtual environments," *Computer Graphics Forum*, vol. 14, no. 3, pp. 29–41, 1995.
- [25] G. Welch and G. Bishop, "Scaat: Incremental tracking with incomplete information," in *Proceedings of the 24th annual conference on Computer graphics and interactive techniques*. ACM Press/Addison-Wesley Publishing Co., 1997, pp. 333–344.
- [26] A. Leardini, L. Chiari, U. D. Croce, and A. Cappozzo, "Human movement analysis using stereophotogrammetry Part 3: Soft tissue artifact assessment and compensation," *Gait & Posture*, vol. 21, pp. 212–225, 2005.
- [27] S. Duprey, L. Chèze, and R. Dumas, "Influence of joint constraints on lower limb kinematics estimation from skin markers using global optimization," *J Biomech*, vol. 43, no. 14, pp. 2858–2862, 2010.
- [28] G. Wu, S. Siegler, P. Allard, C. Kirtley, A. Leardini, D. Rosenbaum, M. Whittle, D. D'Lima, L. Cristofolini, H. Witte, O. Schmid, and I. Stokes, "ISB recommendation on definitions of joint coordinate system of various joints for the reporting of human joint motion - part I: Ankle, hip and spine," *J Biomech*, vol. 35, no. 4, pp. 543–548, 2002.
- [29] E. Grood and W. Suntay, "A joint coordinate system for the clinical description of three-dimensional motions: application to the knee," *J Biomech Eng*, vol. 105, pp. 136–144, 1983.
- [30] D. A. Bowman and L. F. Hodges, "An evaluation of techniques for grabbing and manipulating remote objects in immersive virtual environments," in *Proceedings of the 1997 symposium on Interactive 3D graphics*. ACM, 1997, pp. 35–ff.
- [31] M. Keogh and M. Batt, "A Review Of Femoroacetabular Impingement in Athletes," *Sport. Med*, vol. 38, no. 10, pp. 863–878, 2008.
- [32] M. Leunig, P. E. Beaulé, and R. Ganz, "The Concept of Femoroacetabular Impingement," *Clin Orthop Rel Res*, vol. 467, pp. 616–622, 2009.
- [33] B. Lange, C.-Y. Chang, E. Suma, B. Newman, A. S. Rizzo, and M. Bolas, "Development and evaluation of low cost game-based balance rehabilitation tool using the microsoft kinect sensor," in *Engineering in medicine and biology society, EMBC, 2011 annual international conference of the IEEE*. IEEE, 2011, pp. 1831–1834.
- [34] K. Khoshelham and S. O. Elberink, "Accuracy and resolution of kinect depth data for indoor mapping applications," *Sensors*, vol. 12, no. 2, pp. 1437–1454, 2012.
- [35] C. Charbonnier, S. Chagué, F. Kolo, J. Chow, and A. Lädermann, "A patient-specific measurement technique to model shoulder joint kinematics," *Orthop Traumatol Surg Res*, vol. 100, no. 7, pp. 715–719, 2014.
- [36] T. Sielhorst, C. Bichlmeier, S. M. Heining, and N. Navab, "Depth perception—a major issue in medical ar: evaluation study by twenty surgeons," in *International Conference on Medical Image Computing and Computer-Assisted Intervention*. Springer, 2006, pp. 364–372.
- [37] Y. S. Chang, B. Nuernberger, B. Luan, and T. Höllerer, "Evaluating gesture-based augmented reality annotation," in *3D User Interfaces (3DUI), 2017 IEEE Symposium on*. IEEE, 2017, pp. 182–185.
- [38] T. Sielhorst, M. Feuerstein, and N. Navab, "Advanced medical displays: A literature review of augmented reality," *Journal of Display Technology*, vol. 4, no. 4, pp. 451–467, 2008.
- [39] F. Zhou, H. B.-L. Duh, and M. Billinghurst, "Trends in augmented reality tracking, interaction and display: A review of ten years of ismar," in *Proceedings of the 7th IEEE/ACM International Symposium on Mixed and Augmented Reality*. IEEE Computer Society, 2008, pp. 193–202.
- [40] D. Van Krevelen and R. Poelman, "A survey of augmented reality technologies, applications and limitations," *International Journal of Virtual Reality*, vol. 9, no. 2, p. 1, 2010.
- [41] M. Billinghurst, A. Clark, G. Lee *et al.*, "A survey of augmented reality," *Foundations and Trends® in Human-Computer Interaction*, vol. 8, no. 2-3, pp. 73–272, 2015.